Coherence enhanced intermittency in an optically injected semiconductor laser

A. Campos-Mejía,[1] A. N. Pisarchik,[1*] R. Sevilla-Escoboza,[2] G. Huerta-Cuellar,[2] and V. P. Vera-Ávila[2]

[1] *Centro de Investigaciones en Optica, Loma del Bosque 115, Lomas del Campestre, Leon 37150, Guanajuato, Mexico*

[2] *Centro Universitario de los Lagos, Universidad de Guadalajara, Enrique Díaz de León 1144, Paseo de la Montaña, Lagos de Moreno, Jalisco, Mexico*

apisarch@cio.mx

Abstract: We report on the experimental observation of coherence enhancement of noise-induced intermittency in a semiconductor laser subject to optical injection from another laser at the boundary of the frequency-locking regime. The intermittent switches between locked and unlocked states occur more regularly at a certain value of the injecting laser pump current. A shape of probability distribution of the experimental inter-spike-interval fluctuations is used to quantitatively characterize the intermittent behavior.

OCIS codes: (140.5960) Semiconductor lasers; (190.1450) Bistability; (190.3100) Instabilities and chaos.

References and links

1. D. H. Kawaguchi, K. Inoue, T. Matsuoka, and K. Otsuka, "Bistable output characteristics in semiconductor laser injection locking," IEEE J. Quantum Electron. **21**(9), 1314–1317 (1985).
2. S. Osborne, A. Amann, D. Bitauld, and S. O'Brien, "On-off intermittency in an optically injected semiconductor laser," Phys. Rev. E Stat. Nonlin. Soft Matter Phys. **85**(5), 056204 (2012).
3. D. Ziemann, R. Aust, B. Lingnau, E. Schölland, and K. Lüdge, "Optical injection enables coherence resonance in quantum-dot lasers," Eur. Phys. Lett. **103**(1), 14002 (2013).
4. S. Wieczorek, B. Krauskopf, T. B. Simpsonc, and D. Lenstra, "The dynamical complexity of optically injected semiconductor lasers," Phys. Rep. **416**(1-2), 1–128 (2005).
5. D. O'Shea, S. Osborne, N. Blackbeard, D. Goulding, B. Kelleher, and A. Amann, "Experimental classification of dynamical regimes in optically injected lasers," Opt. Express **22**(18), 21701–21710 (2014).
6. O. Vaudel, N. Péraud, and P. Besnard, "Synchronization on excitable pulses in optically injected semiconductor lasers," Proc. SPIE **6997**, 69970F–1/9 (2008).
7. J. B. Gao, S. K. Hwang, and J. M. Liu, "Effects of intrinsic spontaneous-emission noise on the nonlinear dynamics of an optically injected semiconductor laser," Phys. Rev. A **59**(2), 1582–1585 (1999).
8. A. Campos-Mejía, A. N. Pisarchik, and D. A. Arroyo-Almanza, "Noise-induced on–off intermittency in mutually coupled semiconductor lasers," Chaos Solitons Fractals **54**, 96–100 (2013).
9. Y. Hong, K. A. Shore, J. S. Lawrence, and D. M. Kane, "Wavelength switching by positively detuned side-mode injection in semiconductor lasers," Appl. Phys. Lett. **76**(22), 3170–3172 (2000).
10. Y. Pomeau and P. Manneville, "Intermittent transition to turbulence in dissipative dynamical systems," Commun. Math. Phys. **74**(2), 189–197 (1980).
11. M. Le Berre, E. Ressayre, and A. Tallet, "Type-I intermittency route to chaos in a saturable ring-cavity-retarded differential difference system," J. Opt. Soc. Am. B **5**(5), 1051–1062 (1988).
12. A. D. Staicu, *Intermittency in Turbulence* (Eindhoven University of Technology, 2002).
13. Y.-C. Lai and C. Grebogi, "Intermingled basins and two-state on-off intermittency," Phys. Rev. E Stat. Phys. Plasmas Fluids Relat. Interdiscip. Topics **52**(4), R3313–R3316 (1995).
14. A. N. Pisarchik and V. J. Pinto-Robledo, "Experimental observation of two-state on-off intermittency," Phys. Rev. E Stat. Nonlin. Soft Matter Phys. **66**(2), 027203 (2002).
15. N. Platt, E. A. Spiegel, and C. Tresser, "On-off intermittency: A mechanism for bursting," Phys. Rev. Lett. **70**(3), 279–282 (1993).
16. J. F. Heagy, N. Platt, and S. M. Hammel, "Characterization of on-off intermittency," Phys. Rev. E Stat. Phys. Plasmas Fluids Relat. Interdiscip. Topics **49**(2), 1140–1150 (1994).
17. G. Huerta-Cuellar, A. N. Pisarchik, and Y. O. Barmenkov, "Experimental characterization of hopping dynamics in a multistable fiber laser," Phys. Rev. E Stat. Nonlin. Soft Matter Phys. **78**(3), 035202 (2008).

#234448 - $15.00 USD Received 11 Feb 2015; revised 27 Mar 2015; accepted 30 Mar 2015; published 14 Apr 2015

18. A. N. Pisarchik, R. Jaimes-Reátegui, R. Sevilla-Escoboza, and G. Huerta-Cuellar, "Multistate intermittency and extreme pulses in a fiber laser," Phys. Rev. E Stat. Nonlin. Soft Matter Phys. **86**(5), 056219 (2012).
19. H. Gang, T. Ditzinger, C. Z. Ning, and H. Haken, "Stochastic resonance without external periodic force," Phys. Rev. Lett. **71**(6), 807–810 (1993).
20. A. S. Pikovsky and J. Kurths, "Coherence resonance in a noise-driven excitable system," Phys. Rev. Lett. **78**(5), 775–778 (1997).
21. J. L. A. Dubbeldam, B. Krauskopf, and D. Lenstra, "Excitability and coherence resonance in lasers with saturable absorber," Phys. Rev. E Stat. Phys. Plasmas Fluids Relat. Interdiscip. Topics **60**(6), 6580–6588 (1999).
22. G. Giacomelli, M. Giudici, S. Balle, and J. R. Tredicce, "Experimental evidence of coherence resonance in an optical system," Phys. Rev. Lett. **84**(15), 3298–3301 (2000).
23. O. V. Ushakov, H. J. Wünsche, F. Henneberger, I. A. Khovanov, L. Schimansky-Geier, and M. A. Zaks, "Coherence resonance near a Hopf bifurcation," Phys. Rev. Lett. **95**(12), 123903 (2005).
24. A. M. Yacomotti, M. C. Eguia, J. Aliaga, O. E. Martinez, G. B. Mindlin, and A. Lipsich, "Interspike time distribution in noise driven excitable systems," Phys. Rev. Lett. **83**(2), 292–295 (1999).
25. W.-S. Lam, P. N. Guzdar, and R. Roy, "Effect of spontaneous emission noise and modulation on semiconductor lasers near threshold with optical feedback," Int. J. Mod. Phys. B **17**(22n24), 4123–4138 (2003).
26. J. K. Bhattacharjee and K. Banerjee, "Kramers time in bistable potentials," J. Phys. A **22**(24), L1141–L1146 (1989).
27. B. L. Lan, E. V. Yeoh, and J. A. Ng, "Distribution of detrended stock market data," Fluct. Noise Lett. **9**, 245–257 (2010).
28. H. Wei, H. Xiao-Pu, Z. Tao, and W. Bing-Hong, "Heavy-tailed statistics in short-message communication," Chin. Phys. **26**, 028902 (2009).
29. J. P. Nolan, *Stable Distributions - Models for Heavy Tailed Data* (Birkhuser, 2015).
30. A. M. Segura, D. Calliari, H. Fort, and B. L. Lan, "Fat tails in marine microbial population fluctuations," Oikos **122**(12), 1739–1745 (2013).
31. J. Nolan, "Stable program," http://academic2.american.edu/~jpnolan/stable/stable.html.

1. Introduction

Bistability in semiconductor laser (SL) injection locking was first experimentally demonstrated by Kawaguchi et al. [1] and then numerically simulated using different laser models [2–4]. The two states are associated with two different laser frequencies. One of them is the frequency of the injected light from a master laser, that captures the optical frequency of a slave laser, and the other one is the proper unlocked frequency of the slave laser [5, 6]. Noise is known to play an important role in laser dynamics. There are many sources of noise in laser systems: quantum, electrical, thermal, and mechanical vibration noise. All these noises have different time scales. Spontaneous emission noise, as known [7, 8], substantially modifies laser dynamics; it induces random spikes and intermittent switches between two wavelengths in the bistability domain where deterministic models allow for a single state only, either locking or unlocking [9]. We refer this behavior to noise-induced two-state intermittency.

Among many types of intermittency, only few types are well defined and characterized by specific scaling laws, especially, types I-III and crisis-induced intermittencies [10–12]. Characterization of other types of intermittency, such as, for instance, noise-induced two-state and multistate intermittencies is still under debate and requires further investigation. Two-state intermittency was first predicted by Lai and Grebogi [13] and then experimentally found in a SL [14]. Unlike classical on-off intermittency [15, 16], where the system departures from and approaches towards only one invariant subspace, two-state intermittency requires the existence of at least two invariant subspaces. More complex intermittent behavior, which involves more than two invariant subspaces, so-called multistate intermittency has also been observed in a laser system (see, for example [17, 18],). The regularity of noise-induced pulses in dynamical systems can have non-monotonic character with respect to the noise intensity, optimally correlated to its non-zero value. This phenomenon, referred to as coherence resonance [19, 20], was previously demonstrated theoretically and experimentally in various dynamical systems, including lasers with saturable absorber [21] and optical feedback [22, 23]. Recently, coherence resonance was

#234448 - $15.00 USD Received 11 Feb 2015; revised 27 Mar 2015; accepted 30 Mar 2015; published 14 Apr 2015

predicted in the model of optically injected quantum-dot SLs operated in a frequency-locked regime [3].

In this paper, we present experimental evidence of coherence enhancement of intermittent switches between two different laser wavelengths at the frequency-locking boundary in an optically injected SL. We study how coherence can be enhanced by adjusting the injecting (master) laser pump current. The rest of the paper is organized as follows. In section 2 we describe our experimental setup. In section 3 we analyze optical spectra and time series, and in section 4 we introduce quantitative measures to characterize the coherence and the observed intermittent behavior. Finally, main conclusions are given in section 5.

2. Experimental setup

The experimental setup is shown in Fig. 1. We use two fiber-coupled SLs (Eblana Photonics) stabilized in both the current and the temperature with accuracies of ± 0.01 mA and ± 0.01°C, respectively. An optical isolator (ISO) is inserted between the two lasers to provide unidirectional coupling between the master and slave SLs. The lasers are connected via two 90/10 fiber optical couplers (OC); 90% of the output radiation is used for the coupling through a polarization controller (PC) to ensure parallel polarization, and the remaining 10% is used for signal detection by photodetectors (PD) (Thorlabs PDB 150C, 150-MHz bandwidth). The signal from the photodetector is analyzed with an oscilloscope (Agilent Technologies DSO-X 3102A, 1-GHz bandwidth) and a frequency spectrum analyzer (FSA) (Agilent Technologies EXA N9010A, 9 kHz - 13.6 GHz bandwidth). The threshold currents of the solitary master and slave SLs are 11.5 mA and 12.0 mA at temperatures T = 20.0°C and T = 22.53°C, respectively. The injected power is regulated by an attenuator (Att).The wavelengths of both lasers are monitored using an optical spectrum analyzer (OSA) (ANDO AQ-6315A). The injected light of the master laser enters to the OSA after its reflection from the end of the slave laser. Since the master laser is always in a cw regime, the reflected light has no effect on temporal dynamics recorded by the oscilloscope.

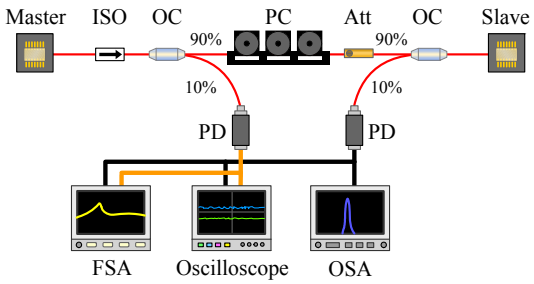

Fig. 1. Experimental setup. PC is a polarization controller, ISO is an optical isolator, OC is an output coupler, Att is an optical attenuator, PD is a photodetector, FSA is a frequency spectrum analyzer, and OSA is an optical spectrum analyzer. The red wire represents the optical fiber, and the black and yellow wires represent the electrical connections.

3. Optical spectrum and time series

During our experiments the slave laser pump current is fixed at I_s = 12.80 mA. Without injection its wavelength is λ_s = 1540.42 nm. The master laser pump current (I_m) is used as a control parameter. A change in I_m leads to approximately linear changes in both the laser power and its wavelength. For 12 mA < I_m < 22 mA the optical frequency of the slave laser is locked by the injected light, i.e. the slave laser emits the radiation with the same wavelength as the master laser. When I_m increases from 22 mA to 27 mA, the wavelength of the master laser increases from λ_m = 1540.58 nm to 1540.64 nm. Despite this slight increase, the slave laser dynamics changes drastically because the control parameter crosses the frequency-locking boundary, i.e. the system leaves the frequency-locking region and the injected light

#234448 - $15.00 USD Received 11 Feb 2015; revised 27 Mar 2015; accepted 30 Mar 2015; published 14 Apr 2015

has no influence on the slave laser anymore. This situation is illustrated in Fig. 2 with the optical spectra and time series. The coincidence of the wavelengths [Fig. 2(a)] means frequency locking and their separation [Figs. 2(b) and 2(c)] means either an intermittent or a free-running regime of the slave laser. At the boundary between the frequency-locking and unlocked regimes, the slave laser intermittently switches between the two wavelengths λ_m and λ_s resulting in jumps between two different values of the slave laser intensity; the value with higher intensity corresponds to the frequency-locking regime and with lower intensity to the unlocked regime.

When 22 mA < I_m < 24 mA the slave laser remains most of the time in the frequency-locking regime (higher intensity level), occasionally jumping to the unlocked state (lower intensity level), as seen in Figs. 2(d) and 2(g). Around I_m = 24.6 mA the switches occur more regularly with an average switching frequency of 3.7 MHz [Figs. 2(e) and 2(h)]. At I_m = 25.4 mA the slave laser remains most of the time in the unlocked state, presenting occasional switches to the locked state [Figs. 2(f) and 2(i)]. For I_m > 26.0 mA the slave laser emits again a stable radiation being outside the frequency-locking region. Thus, the slave laser emission presents two well-defined stable states and the intermittency region between them. Such a behavior is illustrated in Fig. 3(a) with the bifurcation diagram of the slave laser peak intensity. To obtain this diagram we analyzed 501 time series, each 1-ms long and comprised of 500000 points, recorded for the driving currents from I_m = 20 mA to 28 mA with a step of 0.02 mA. In the diagram, one can clearly distinguish each one of the two stable states and the intermittency region between 22 mA and 26 mA.

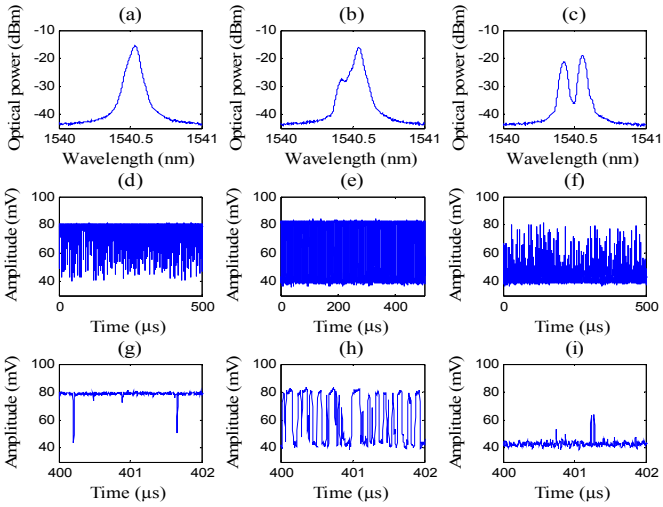

Fig. 2. (a-c) Average optical spectra recorded by OSA and (d-i) oscilloscope traces for (a,d) I_m = 22.0 mA, (b,e) 24.6 mA, and (c,f) 25.4 mA. The lower row (g,h,i) is the zoomed parts of the above time series.

Figure 3(b) shows the evolution of the optical spectrum of both lasers recorded by the OSA. The color shows the maximum power of the optical spectral components. For small pump currents of the master laser (I_m < 11.5 mA), i.e. below the laser threshold, only the wavelength of the slave laser (λ_s = 1540.4 nm) is presented in the spectrum, and it is independent of I_m. At I_m = 11.5 mA the master laser reaches the lasing threshold and locks the slave laser frequency, i.e. $\lambda_s = \lambda_m$ for 12 mA < I_m < 21 mA [the single sloping line in Fig. 3(b)]. For larger currents (21 mA < I_m < 26 mA) the slave laser exhibits the intermittent behavior. When the difference between λ_s and λ_m is smaller than the OSA spectral resolution (± 0.05 nm), the local maximum at λ_s does not appear in the optical spectrum. This results in

#234448 - $15.00 USD Received 11 Feb 2015; revised 27 Mar 2015; accepted 30 Mar 2015; published 14 Apr 2015

the approximately 0.05-nm width of the lines in the diagram. When the separation between the lines corresponding to the master and slave laser wavelengths is large enough, we are able to distinguish two peaks in the spectrum, as in Fig. 2(b). If not [as in Fig. 2(a)], we can only decide that the laser switches between the two wavelengths by observing the time series recorded with the oscilloscope. Finally, for I_m > 26 mA each laser emits at its own free-running frequency. For high currents, the two lines in Fig. 3(b) represent two independent wavelengths, the upper one corresponds to λ_m, which increases with I_m, and the lower one, fixed at 1540.4 nm, corresponds to the free-running frequency of the slave master.

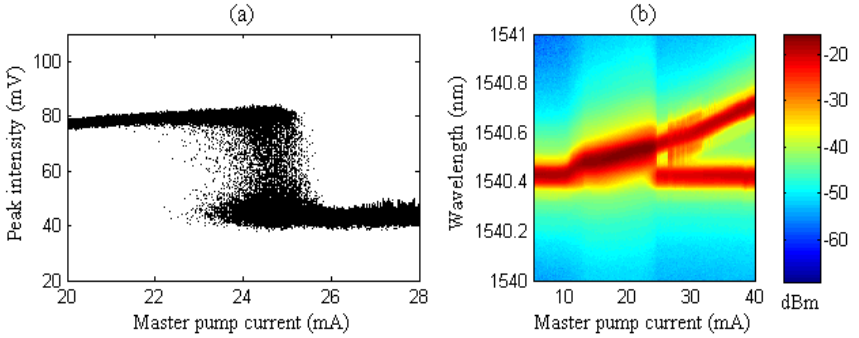

Fig. 3. (a) Bifurcation diagram of slave laser peak intensity frequency-locking boundary and (b) local maxima recorded by OSA.

To test the reproducibility of the diagrams in Fig. 3, we performed the measurements many times and obtained the same behavior. We should note that the injected power is too small to induce chaos in the slave laser. The spiking and switching dynamics at the frequency-locking boundary has a stochastic origin due to internal noise.

4. Coherence enhancement

The observed intermittent behavior is known to be induced by noise inherent to SLs (see, e.g., [3, 7]). The noisy behavior of the laser emission is clearly seen in Fig. 3(a) as broaden widths of the upper and lower branches of the bifurcation diagram. In the bistability domain, the system behavior can be presented in the form of a double-well potential with a current-dependent shape. Unlike coherence resonance, which is characterized by increasing regularity with respect to noise, in our case the noise is almost constant and the regularity is optimized for a certain value of the master laser current when the double-well potential is more symmetric. On-off intermittency is typically defined by conditions for the onset of intermittent behavior, namely, the distribution of laminar phases and the mean laminar phase versus a control parameter, usually noise intensity [16]. Since our laser displays either separate spikes, like those in Figs. 2(g) and 2(i), or switches between two equilibriums, like those in Fig. 2(h), it is impossible to measure the duration of the turbulent phase and hence characterize this type of intermittency by commonly used scaling relations. Therefore, similar to neuron systems, we measure inter-spike-intervals (ISI) between consecutive optical spikes or switches, evaluated by $\Delta T_i = t_{i+1} - t_i$, with t_i being the instant of time when a spike occurs. Although the ISI distribution has been the subject of many studies [24, 25], to the best of our knowledge, the ISI fluctuations Δ_n for this system have not been yet considered. The ISI fluctuations are defined as the difference between successive natural logarithms:

$$\Delta_n = \ln\left(\Delta T_{i+1}\right) - \ln\left(\Delta T_i\right). \quad (1)$$

To find Δ_n in the intermittency region of our system, we analyze the time series and measure ΔT_i as the spike intensity crosses the value of 60 mV. This value is selected because it lies at the middle of the two system states. For spikes whose intensity does not cross the value of 60

#234448 - $15.00 USD Received 11 Feb 2015; revised 27 Mar 2015; accepted 30 Mar 2015; published 14 Apr 2015

mV, ΔT_i is calculated as the distance between the consecutive local minima or local maxima. The current dependence of the standard deviation (SD) of Δ_n in the intermittency region, shown in Fig. 4(a), displays a minimum around 24.5 mA meaning that the system dynamics exhibits maximum coherence. It should be noted that small variations of the current threshold do not produce qualitative changes in Δ_n.

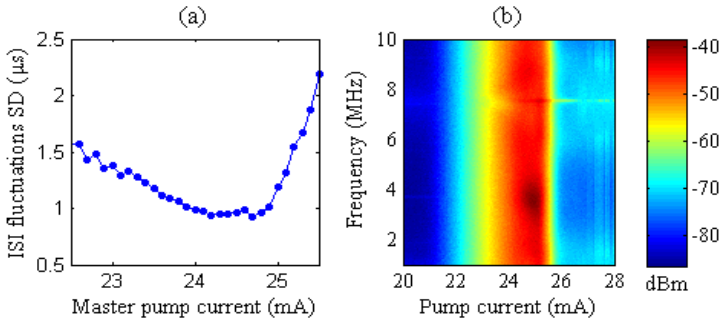

Fig. 4. (a) Standard deviation of inter-spike-interval fluctuations in intermittency region and (b) power spectrum as a function of master laser pump current. The minimum in (a) and the dark spot in (b) correspond to maximum coherence.

Another quantitative measure of the coherence is the power of the dominant spectral component in the frequency spectrum. The higher the power at a particular frequency, the more regular dynamics is. Figure 4(b) shows the power spectrum as a function of I_m. The dark spot in the vicinity of 25 mA means that the laser behavior for this pump current is more regular than for other currents, because of the existence of the dominant frequency of about 3.7 MHz at which the power is significantly higher than for other spectral components. This frequency is probably related to the Kramers time in the bistable potential [26]. Another, but no so pronounced maximum occurs at the second harmonic of this frequency.

Next, we will show that the intermittent behavior can be characterized with probability distribution of the ISI fluctuations. In particular, we find that the observed spiking behavior obeys a non-Gaussian stable distribution, a class of probability distributions allowing skewness and heavy tails, i.e. tails that are "heavier" than an exponential. This means that events, which are far from the average, appear more frequently than in a Gaussian case. Heavy tailed distributions were found in different areas, from economics and finance to engineering and biology [27–30]. General stable distributions allow for varying degrees of tail heaviness and skewness, and are characterized by four parameters: an index of stability or characteristic exponent $\alpha \in (0,2]$, a skewness parameter $\beta \in [-1,1]$, a scale parameter $\gamma \geq 0$, and a location parameter δ. The parameter α is an indicator of the tails. For $\alpha = 2$ the distribution is Gaussian, and smaller values imply heavier tails. For $\beta = 0$ the distribution is symmetric, and a different value means that the distribution is skewed either to the left or to the right, depending on the sign. The parameter γ is an indicator of the distribution width. The parameter δ translates the distribution horizontally, accordingly to its value. Since α and β determine the distribution form, they may be considered as shape parameters. The fitted stable parameters of this kind of probability distributions are showing to be a useful tool to quantify and monitor the state of complex systems. To fit the ISI fluctuations we use the computer program STABLE [31] based on the maximum likelihood method for estimation of stable parameters. The probability density, obtained with a Gaussian kernel [30] for the experimental data is compared with the fitted stable probability density.

The stable model is acceptable if there is a good agreement between the fitted stable density and the smoothed data density. We find that the smoothed data density of the experimental ISI fluctuations is in good agreement with the fitted stable density for the range of pump currents. The stable fitted parameters α and γ in the intermittency region plotted

#234448 - $15.00 USD Received 11 Feb 2015; revised 27 Mar 2015; accepted 30 Mar 2015; published 14 Apr 2015

with the 95% confidence interval are shown in Fig. 5. We can see that at the center of the intermittency region α is very close to 2 (α = 1.99), and before and after this region the characteristic exponent is around 1.9. In this case, as $\alpha > 1.9$ the parameter β has no effect on the shape of the distribution. The parameter γ represents essentially the same behavior as the SD of the ISI fluctuations, since it is related with how spread the distribution is. The parameter δ is practically zero for all pump currents.

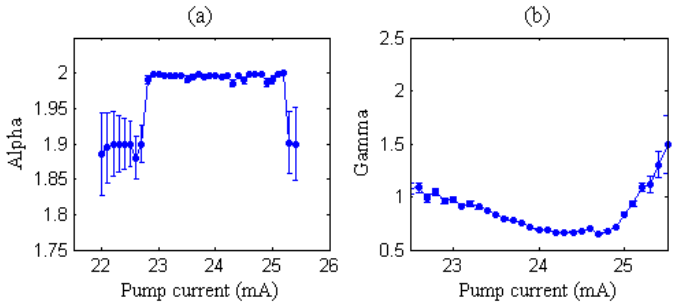

Fig. 5. Fitted stable parameters (a) α and (b) γ as a function of the master laser pump current. The 95% confidence intervals are plotted.

The results presented in Fig. 5 suggest that the fitted stable parameters α and γ can be used to quantify the intermittent behavior in the laser. The non-smooth dependence of α on I_m means the existence of two fluctuation states, the one obeys a non-Gaussian stable distribution, which is heavy tailed, and the other one obeys a Gaussian stable distribution. The two abrupt changes in Fig. 5(a) occur at the bifurcation points I_m = 22.8 mA and 25.2 mA, where the laser changes its behavior, respectively, from one-state on-off intermittency to two-state intermittency and back. The fluctuation state with smaller α (heavy density tails) means higher probability for large ISI fluctuations, whereas the fluctuation state with $\alpha \approx 2$ implies a normal distribution. Therefore, the parameter α can serve as an indicator of the type of intermittency. Since γ is an indicator of the distribution width, the larger the ISI fluctuations, the wider the distribution is. Therefore, the dependence of γ on I_m in Fig. 5(b) almost replicates the dependence in Fig. 4(a); minimum γ indicates maximum coherence.

5. Conclusion

In this work we have presented experimental evidence of coherence enhancement of noise-induced two-state intermittency in an optically injected SL at the boundary of the frequency-locking regime. With the bifurcation diagrams of the laser peak intensity and the optical spectral components we have demonstrated the existence of intermittent switches between the frequency-locking and unlocked regimes. The minimum in SD of the ISI fluctuations has indicated the existence of an optimal master laser pump current for highest coherence of the intermittent jumps. Furthermore, the power spectrum exhibited the prevalence of a particular spectral component or the existence of a dominant frequency, which is probably related to the Kramers time. We have associated this phenomenon with an improvement in the symmetry of the double-well potential. We have also found that the ISI fluctuations in the intermittency regime obeyed two different probability distributions, a non-Gaussian stable distribution (heavy tailed) for the spiking behavior near one equilibrium state, and a normal distribution for the random switches between the two states, quantified by fitted stable parameters α and γ. The stable fit can be used to select adequate models and parameters for simulating intermittent dynamics by comparing the fitted stable parameters obtained from experimental and numerical data.

#234448 - $15.00 USD Received 11 Feb 2015; revised 27 Mar 2015; accepted 30 Mar 2015; published 14 Apr 2015